Published March, 2011

An Investigation of the Kinetic Processes Influencing Mercury Emissions from Sand and Soil Samples of Varying Thickness

Jason L. Quinones and Anthony Carpi*

Mercury flux from $HgCl_2$—treated sand and untreated soil samples of varying thickness (0.5–15 mm) were measured in dark and light under a Teflon dynamic flux chamber. Mean emissions over a 5.5-d sampling period showed an increase with depth for sand samples between 0.5 and 2 mm, but increasing depth above 2 mm had no effect. First-order kinetic models showed strong goodness of fit to the data and explained a high degree of variability in the emissions profile of all sand samples (R^2 = 0.70–0.98). Soil samples showed an initial emissions peak that was not correlated with depth, suggesting a very shallow process at work. However, longer-term "baseline" emissions, measured as mean emissions between Days 4.5 and 5.5, did show a relationship with depth. First-order kinetic models showed good fit for soil samples up to 4 mm thick (R^2 = 0.66–0.91); however, thicker samples did not show a consistent fit to first- or second-order kinetic models (1° R^2 = 0.00–0.46; 2° R^2 = 0.00–0.54). The data suggest that mercury emissions from soil samples may follow a multicomponent model for which more than one component is affected by incident radiation.

J. Environ. Qual. 40:647–652 (2011)
doi:10.2134/jeq2010.0327
Posted online 31 Jan. 2011.
Freely available online through the author-supported open-access option.
Received 21 July 2010.
*Corresponding author (acarpi@jjay.cuny.edu).

5585 Guilford Rd., Madison, WI 53711 USA

Divalent mercury (Hg^{2+}) in soil and water surfaces can be reduced to elemental mercury (Hg^0) and emitted to the atmosphere (Wood, 1974; Schlüter et al., 1995; Fitzgerald et al., 1998; Wang et al., 2003). Environmental factors, such as temperature (Siegel and Siegel, 1988), UV light (Moore and Carpi, 2005; Xin et al., 2007), humic acid concentration (Mauclair et al., 2008), pH, and moisture (Schuster, 1991; Schlüter, 2000; Song and Van Heyst, 2005), have been shown to influence this process. Despite progress in Hg research, little is known about the exact mechanism of reduction and emission from soil, including the soil depth to which Hg emissions can be attributed. One factor that appears to play a dominant role in the reduction of Hg in soil is light energy (Carpi and Lindberg, 1997; Zhang et al., 2001; Gustin et al., 2002), and especially ultraviolet light (Bonzongo and Donkor, 2003; Moore and Carpi, 2005; Xin et al., 2007). Hence, the penetration of light into soil may have a significant effect on Hg emission, and understanding emissions from soil of various depth should provide data to help understand the mechanisms involved. Carpi and Lindberg (1997) and Feng et al. (2006) have suggested that the top 1 to 2 cm and 0 to 5 cm of soil, respectively, are of most importance in this process, whereas others, such as Dreher and Follmer (2004), have demonstrated that the upper 0 to 8 cm of soil contains the highest concentration of total Hg. Almeida et al. (2005) have shown that Hg loss from forest soil after conversion from forest to pasture was most significant in the surface 20 cm of soil. Hintelmann et al. (2002) found that newly deposited Hg is more easily lost through volatilization, suggesting a shallow surface emissions phenomenon. Divis et al. (2005) have suggested that Hg emissions from marine and river sediment may be limited to the upper 0 to 4 cm because their data showed large spikes in total and labile Hg in the surface Fe and Mn reduction zone. However, understanding emissions of Hg from varying depths of soils requires further investigation. In this work, we describe a series of laboratory experiments conducted to investigate emissions from substrates of different thicknesses used to simulate surface depth.

Materials and Methods

Samples

Samples were created using clean laboratory grade SiO_2 sand (Sigma-Aldrich, St. Louis, MO) or with soil collected from a small forested area in southwestern Connecticut. All sand samples were

Dep. of Sciences, John Jay College, The City Univ. of New York, 445 West 59th St., New York, NY 10019. Assigned to Associate Editor Rainer Schulin.

baked for approximately 3.5 h at 300°C using a Fisher Isotemp 800 oven (Fisher Scientific, Pittsburgh, PA) before treatment and analysis to ensure background Hg did not pose an experimental bias during analysis. Sand samples were amended with an $HgCl_2$ solution to a final Hg concentration of 0.005 ppm Hg by mixing 1 mL of a 0.5-ppm $HgCl_2$ solution with 23.5 mL of Milli-Q water per 100 g of SiO_2 sand. All sand samples were analyzed in triplicate using a DMA 80 Direct Mercury Analyzer (Milestone, Sorisole, Italy) after $HgCl_2$ treatment, and final sand concentrations were averaged 0.0052 ± 0.0003 ppm. Sand was mixed with the Hg solution in a 100-mL flask and then transferred to a clean Teflon sheet. Doped sand samples were spread evenly with a Teflon spatula to create a circle with a diameter of 23 cm (surface area of 0.04154 m^2). The doping process may have affected Hg speciation because $HgCl_2$ is known to hydrolyze in water to $Hg(OH)_2$ and HgClOH (Ciavatta and Grimaldi, 1968). However, this is an equilibrium process that reverses on evaporation of water. Although this does not preclude the formation of the other complexes of Hg from trace impurities present despite the fact that clean sample handling and preparation procedures were used, the behavior of Hg in these doped sand samples mimicked that of other studies in our laboratory in which dry $HgCl_2$ was placed under our chamber.

Soil was collected from underneath the litter of a small forested area in southwestern Connecticut. Soil in the area falls into the Paxton soil series and is considered a fine sandy loam derived from parent material of coarse-loamy lodgment till (USDA, 2010). The area has been in residential, suburban use since 1927 and was used as pasture before this date. No direct waterborne or airborne source of Hg exists within a 2-km radius of the site, and the nearest urban area (Norwalk, CT) is 5 km southeast of the site. Soil was collected from the upper 7 to 8 cm of topsoil within an approximately 0.5 m^2 plot. Samples of the collected soil (~500 g) were sent to Cornell University Nutrient Analysis Laboratory (Ithaca, NY) for characterization and were found to have a moisture content of 7.5%, a pH in water of 5.7, and an organic matter content of 21.6%. The soil displayed trace levels of naturally occurring metals within normal limits. Soil was air dried at room temperature, sieved using a USA Standard Test Sieve ASTM E-11, and homogenized by mixing it inside a clean polyethylene bucket with a clean Teflon spatula. Soil collected was not amended with $HgCl_2$ and thus was tested for its native Hg content. Soil was analyzed with the Milestone DMA 80 Direct Mercury Analyzer, and the average concentration of Hg in the samples was 0.156 ± 0.031 ppm.

Given the difficulty in creating very thin samples of sand or soil, samples were created by taking a known mass of substrate and spreading this to a consistent surface area (0.04154 m^2). Sample masses were chosen systematically, and then thickness was measured using a General Ultra-tech stainless steel digital caliper with a 0.01 mm resolution and a range of 0 to 150 mm (Cole-Palmer, Vernon Hills, IL). To measure thicknesses, two uniform glass surfaces were sandwiched above and below the individual sand and soil samples. The thickness of the glass surfaces and the Teflon sheet was subtracted from the total thickness measured for each sample (depth). Sand samples with the following thickness (and mass) were measured: 0.54 mm (17 g sand), 0.88 mm (25 g), 1.35 mm (50 g), 2.07 mm (75 g), 2.39 mm (100 g), 3.05 mm (150 g), and 5.42 mm (300 g). Thickness (and mass) of soil samples were varied as follows: 1.97 mm (17 g), 3.28 mm (50 g), 4.60 mm (75 g), 5.62 mm (100 g), 6.92 mm (150 g), 8.33 mm (175 g), 9.52 mm (200 g), 11.63 mm (300 g), 15.51 mm (400 g). We were unable to create soil samples with adequate surface coverage that were less than 2 mm thick due to the tendency of soil particles to aggregate. Before running each sample, chamber blanks were measured using clean Teflon sheets to account for any chamber artifacts. Blanks throughout the sampling period were measured under continuous full spectrum light and showed an average flux of 6.56 ± 0.25 ng h^{-1} m^{-2}, where the error reported is a 95% confidence interval. Although the blanks are higher than reported in other studies, blank measurements were consistent throughout the study and did not affect the relative comparisons of fluxes in this work.

Flux Measurement and Apparatus

Flux measurements were made using a semispherical Teflon dynamic flux chamber with a 23.5-cm internal diameter and an internal volume of approximately 2.5 L. Mercury fluxes were measured at a continuous flow rate of 6 L min^{-1}. Outlet and inlet concentrations were accurately analyzed by a Tekran Mercury Vapor Analyzer (model 2537A; Tekran Instruments Corp. Knoxvill, TN) as described by Lindberg and Price (1999) and Lindberg and Meyers (2001).

Elemental Hg was measured as sequential 5-min concentrations, with two inlet and two outlet measurements alternating in sequence for one full cycle of 20 min resulting in two sequential flux readings. All flux calculations are represented as an average of the two sequential readings collected during the 20-min cycle. The Tekran Analyzer was calibrated weekly using an external injection source (10 μL) and daily using the Tekran's internal permeation source. The internal and external calibrations displayed less than a 10% difference throughout the study. All samples were analyzed in a vertical laminar flow hood fitted with HEPA and activated-carbon filters to limit ambient Hg inside the hood.

Chamber inlet and outlet Hg concentrations were used to calculate fluxes using the steady-state flux equation:

$$F = [(C_o - C_i)\ (A^{-1})]Q \quad [1]$$

where C_o and C_i are the outlet and inlet concentrations, respectively (ng m^{-3}); A is the surface area of the sample being measured (m^2); Q is the flushing flow rate (m^3 h^{-1}); and F is the steady-state flux (ng h^{-1} m^{-2}) as per Zhang et al. (2001).

Temperature and Light

Temperature and light were monitored daily. The temperature of the sample surfaces was measured using a 675-nm laser infrared thermometer (Fisher Scientific) with a SD of ±2°C. Temperatures were consistent throughout experiments, ranging from 45 to 52°C with an average of 49°C for sand sample surfaces. A NESLAB-RTE 10 cooling system (Thermo Scientific, Worcester, MA) was added to the experimental setup during analysis of soil samples. The tray containing the samples was placed on a coiled copper pipe as per Mauclair et al. (2008).

Cool water was circulated through the pipe to maintain the temperature of the soil samples at 32°C with a SD of ±7°C across the diameter of the sample surface. Light was supplied by broad-spectrum Multi Vapor metal halide lamps (GE, Cleveland, OH) placed approximately 46 cm above the samples. The lamp produces radiation in the UV, visible, and infrared regions that closely mimic the solar spectrum. Light intensity was measured as a function of wavelength, with the greatest intensities being associated with the 500- to 600-nm range. Light intensities ranged from 70 to 100 w m^{-2} over the surface of the sample, with the lower intensity being the average of measurements taken at the edge of the samples and the higher intensity being the average measured at the center of the samples. All light intensities were measured using an LI-250A Light Meter Quantum/Radiometer/Photometer with an accuracy of ±2% (LI-COR Biosciences, Lincoln, NA).

Results

Fluxes were measured for 14 Hg-amended sand samples and 16 non-amended natural soil samples held under dark and light conditions. No difference in flux was noted between samples of different thicknesses in the dark. Emissions from sand samples in the dark averaged –0.95 to 0.44 ng m^{-2} h^{-1}, and no significant trends were noted over the 3-d dark sample periods. Emissions from soil samples in the dark averaged –0.55 ± 0.32 ng m^{-2} h^{-1}, and no significant trends were identified over the 3-d dark sample periods. All samples showed an immediate increase in Hg emission on the introduction of light, with flux maxima occurring at the onset of light exposure (Fig. 1). All samples exhibited a gradual decline in flux on continuing light exposure. All samples were exposed to light for a minimum of 5.5 d (132 h), and flux values during this 132-h exposure period were averaged for each sample to empirically compare sample emissions. For the thinnest sand samples (up to 2 mm), an increase in Hg flux was seen with increasing thickness; however, no statistically significant difference in average flux was seen for samples thicker than 2 mm (Fig. 2). Replicate sand samples showed good agreement with one another (Fig. 2).

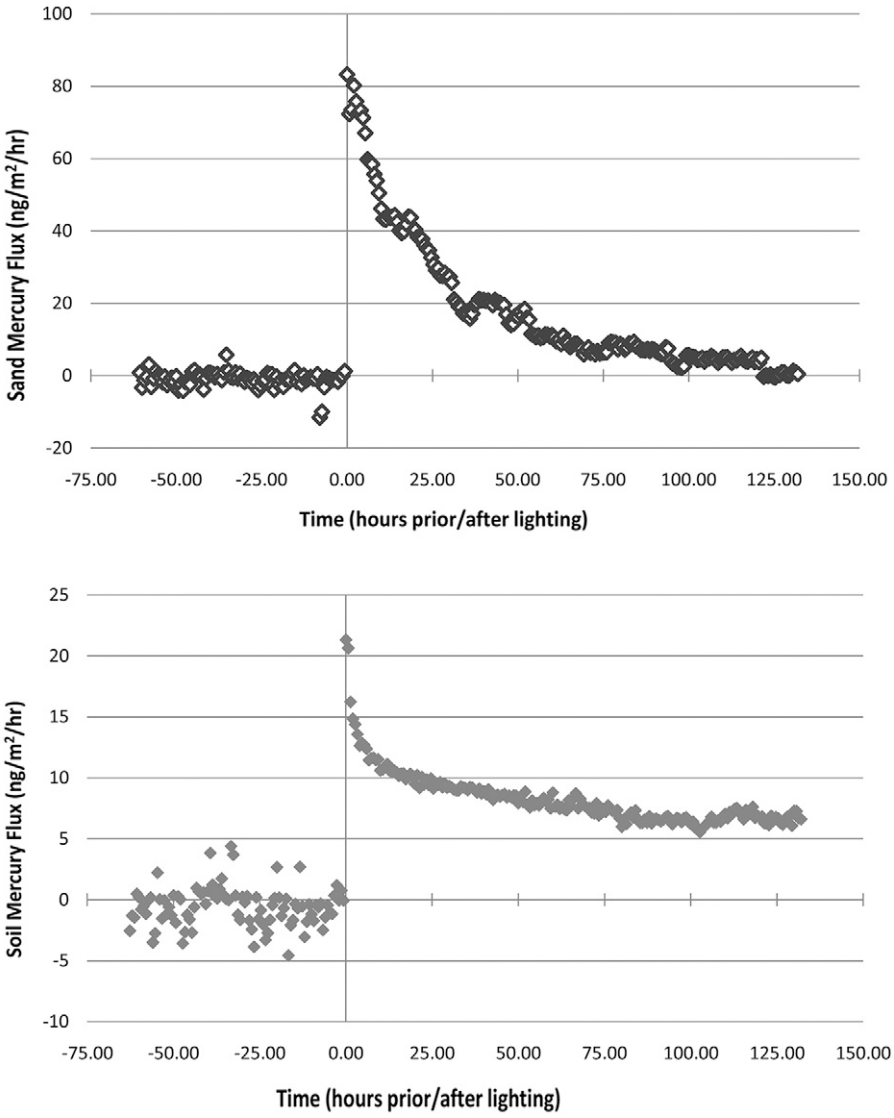

Fig. 1. Graph of Hg flux from representative 17 g sand (open diamond) and soil (closed diamond) samples. No difference in flux was noted in the dark; however, an immediate and dramatic increase in flux was seen on exposure to light (time = 0), and flux slowly decreased with continued exposure to light.

Soil samples consistently showed significantly lower Hg emission levels than sand samples despite higher concentrations of total Hg (0.156 ± 0.031 vs. 0.0052 ± 0.0003 ppm in soil and sand, respectively). Like sand, replicate soil samples showed good reproducibility (Fig. 3). Mean soil Hg flux did not show a significant relationship with sample thickness (Fig. 3). Two of the three thickest soil samples (one 11.63-mm sample and the 15.51-mm sample) exhibited average fluxes that were significantly higher at the 95% confidence level than all other samples; however, the relationship between thickness and average flux among all samples was weak (R^2 = 0.21).

To explore the possible mechanisms of Hg emission from the samples, zero-, first-, and second-order kinetic models were fit against the data. For the majority of sand samples, the first-order model was the best fit and took the form $[F] = [F]_0 e^{-kt}$, where F is flux, $[F]_0$ is the flux at time (t) = 0, and k is rate constant of the process in hours. Values for $[F]_0$, k, and R^2 were calculated for each sand sample and are shown in Table 1. The second-order model fit was determined by calculating R^2 values for best fitting line to the data plotted as $1/[F]$ versus t; these values are listed in Table 1. The first-order model consistently outperformed the second-order model for the thinnest sand samples. The thickest sand samples showed good fit to first- and second-order models; however, R^2 values for second order models were slightly higher (Table 1). Half-times ($t_{1/2}$) were

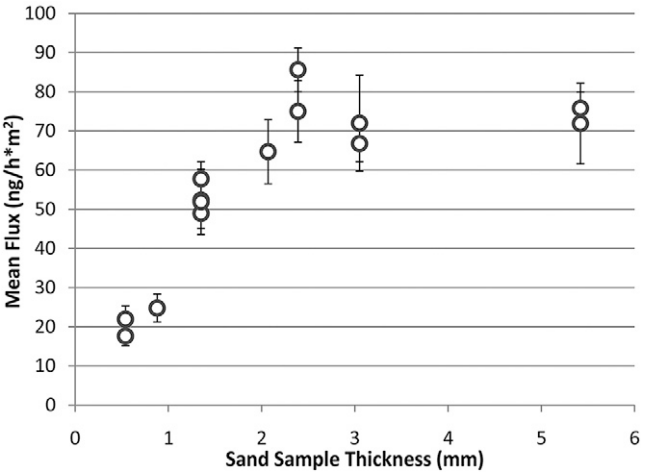

Fig. 2. Mean Hg flux ± 95% CIs from sand samples (ng h^{-1} m^{-2}) versus thickness of sample in millimeters. Each point represents the statistical average of Hg emissions collected during a sampling interval of 5.5 d in which the sample was exposed to full-spectrum light; 95% confidence intervals are shown as error bars. Replicate trials were run for most samples. Flux increased proportional to thickness up to ~2 mm but showed no significantly significant difference (α = 0.05) above this depth.

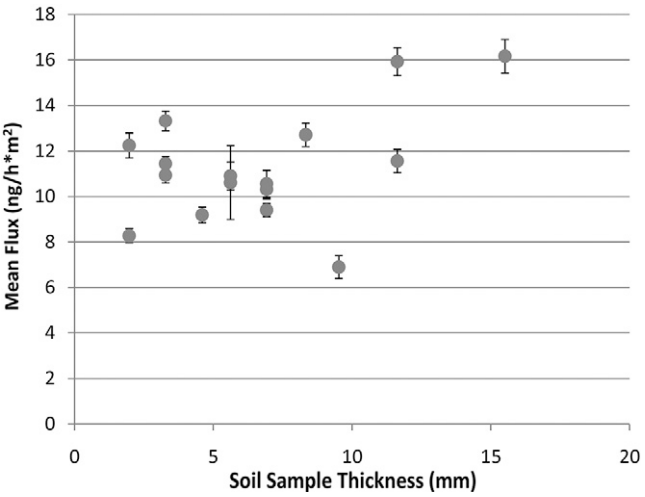

Fig. 3. Mean Hg flux ± 95% CI from soil samples (ng h^{-1} m^{-2}) versus thickness of sample (mm). Each point represents the statistical average of Hg emissions collected during a sampling interval of 5.5 d in which the sample was exposed to full-spectrum light; 95% CIs are shown as error bars. Replicate trials were run for many samples. The thickest samples have slightly higher average fluxes; however, the R^2 value for the goodness of fit for a trend line with thickness is quite low (0.21).

calculated for each sample from the experimentally determined rate constants and are shown in Fig. 4. Half-times tended to increase with increasing sample thickness (R^2 = 0.44) (Fig. 4), but this change appears to level off for the thickest samples. The thinnest sand samples (0.54 mm) produced an emissions decay curve that approached zero; however, thicker sand samples approached an emissions asymptote above zero. To quantify and compare these longer-term "baseline" emission levels, sand flux values during the final 24 h of each sample's exposure to light (Days 4.5–5.5) were averaged (Fig. 5). Baseline fluxes of Hg from sand samples show a clear relationship with increasing depth (R^2 = 0.62); however, this trend appears to level off

Table 1. First-order kinetic model parameters for sand samples with coefficients of determination for first- and second-order best-fitting models.

Thickness	$[F]_0$†	k	First-order R^2	Second-order R^2
mm	ng h^{-1} m^{-2}	h^{-1}		
0.54	76.6	0.0278	0.92	0.36
0.54	67.7	0.0290	0.83	0.12
0.88	69.2	0.0129	0.89	0.83
1.35	99.0	0.0127	0.88	0.78
1.35	120.9	0.0152	0.95	0.86
1.35	117.4	0.0165	0.90	0.96
1.35	128.9	0.0144	0.98	0.86
2.07	169.8	0.0197	0.88	0.89
2.39	142.7	0.0121	0.85	0.96
2.39	135.0	0.0080	0.76	0.83
3.05	140.3	0.0136	0.83	0.94
3.05	108.4	0.0085	0.79	0.87
5.42	129.6	0.0123	0.70	0.82
5.42	116.5	0.0074	0.75	0.81

† Flux at time 0.

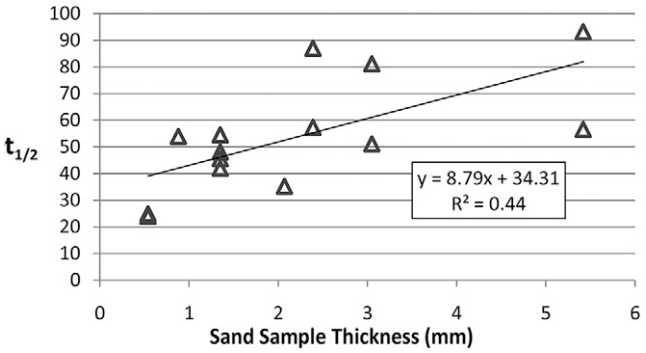

Fig. 4. Emission half-times calculated for sand samples using experimentally determined rate constants.

among the thicker sand samples, consistent with the observed increase in emission half-times.

For soil samples (Table 2), the first-order model appears to fit the data reasonably well for the thinnest samples. However, soil samples >4 mm thick showed only sporadic and weak fit to first- and second-order models. Half-time values for soil were higher than for sand; however, $t_{1/2}$ values for soil showed no relationship with sample thickness (Fig. 6). All soil samples approached an emissions asymptote at positive values regardless of sample thickness. Soil flux values during the final 24 h of each sample's exposure to light (Days 4.5–5.5) were averaged to compute baseline flux levels (Fig. 7). Baseline fluxes over soil in light remained significantly elevated at the 95% confidence level over soil fluxes in dark. Baseline soil fluxes in light showed a weak relationship with sample thickness (R^2 = 0.39), and samples >10 mm thick had baseline emissions that were significantly elevated over all other samples at the 95% confidence level.

Discussion and Conclusions

Mercury emissions from all samples were affected by incident radiation. At the shallowest depths measured, emissions from sand samples increased with sample thickness. Emissions from

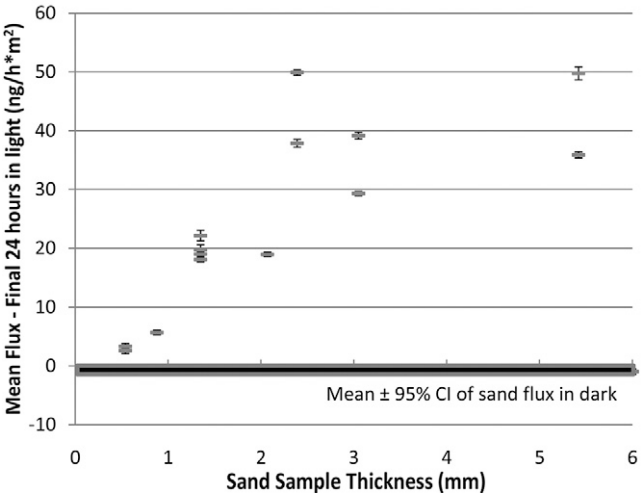

Fig. 5. Mean Hg flux ± 95% CI from sand samples (ng h^{-1} m^{-2}) during their final 24 h of exposure to light. Mean ± 95% CIs of sand flux from sand in dark shown at bottom.

Table 2. First-order kinetic model parameters for soil samples with coefficients of determination for first- and second-order best-fitting models

Thickness	$[F]_0$†	k	First-order R^2	Second-order R^2
mm	ng h^{-1} m^{-2}	h^{-1}		
1.97	17.1	0.005531	0.79	0.91
1.97	11.3	0.005133	0.76	0.81
3.28	17.2	0.004182	0.73	0.83
3.28	14.3	0.003557	0.66	0.71
3.28	15.0	0.005097	0.85	0.86
4.6	10.7	0.002559	0.31	0.38
5.62	10.0	0.001330	0.02	0.01
5.62	11.6	0.001396	0.07	0.06
6.92	13.2	0.004042	0.37	0.44
6.92	9.3	0.000223	0.00	0.00
6.92	12.8	0.003633	0.45	0.54
8.33	15.1	0.003041	0.31	0.33
9.52	10.3	0.007485	0.46	0.08
11.63	11.7	0.000984	0.01	0.01
11.63	19.1	0.003099	0.35	0.37
15.51	20.2	0.003857	0.43	0.52

† Flux at time 0.

sand samples thicker than 2 mm did not show a consistent relationship with thickness. Mercury emissions from soil samples did not show a consistent relationship with sample thickness at any depth, although a slight upward trend is noted in the data. The relationship between flux and thickness identified in shallow sand systems may be related to light penetration. Light penetration at 1 mm has been found to be 80% in SiO_2 sand but <2% in sediment. At 2 mm, light penetration drops to 52% for SiO_2 and 0% for sediment, and light penetration is only 9% by 4 mm in SiO_2 sand (Gomoiu, 1967).

Mercury emissions in light from all sand samples show good fit to a first-order kinetic model, suggesting a concentration-dependent process. The intercept of the first-order model, $[F]_0$, was depth related for samples up to 2 mm thick but was depth independent for thicker samples, suggesting that initial emissions are strongly influenced by processes penetrating the first

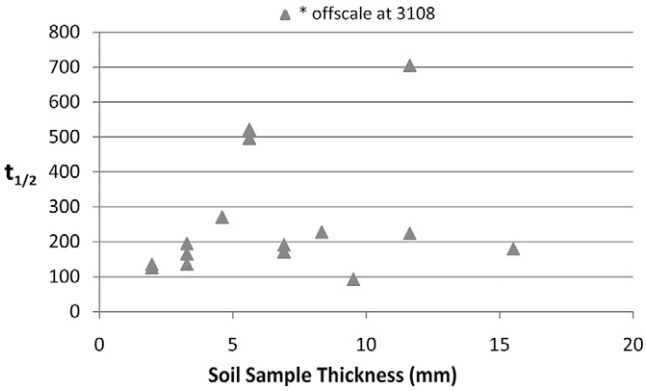

Fig. 6. Emission half-times calculated for soil samples using experimentally determined rate constants.

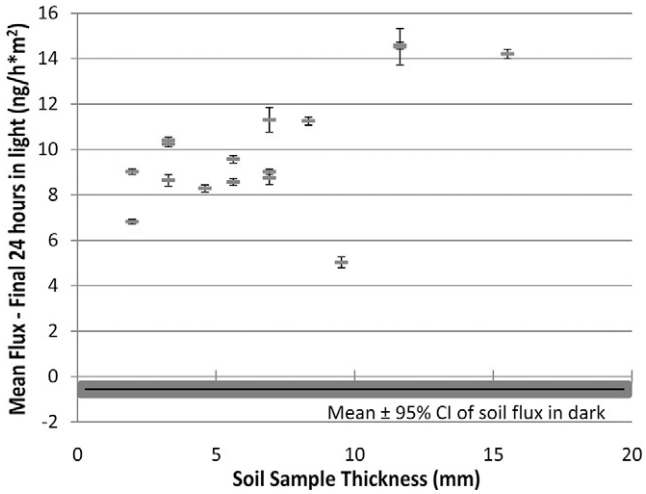

Fig. 7. Mean Hg flux ± 95% CIs from soil samples (ng h^{-1} m^{-2}) during their final 24 h of exposure to light. Mean ± 95% CIs of soil flux from soil in dark shown at bottom.

2 mm of sand and are likely due to the direct reduction of surface-adsorbed Hg by light in these layers. Emissions levels dropped sharply within the first 36 to 48 h for all sand samples and then entered a longer period of gradual "baseline" decline, remaining elevated over Hg emissions from sand in the dark. These baseline emission levels are correlated with increasing depth across all samples measured, suggesting that the latter portion of the emissions profile may be dominated by a secondary process of replenishment or direct emission from deeper layers of substrate.

Mercury emissions in light from soil samples up to 4 mm thick show good fit to a first-order kinetic model, suggesting a concentration-dependent process in the upper layer of soil systems. The first-order kinetic model intercept, $[F]_0$, was not correlated with depth for soil samples, suggesting that the initial flux peak is dominated by a very shallow process limited to the upper surface of soil particles. These initial flux peaks from soil samples were limited to a shorter period than sand samples (generally 10–12 h). Soil samples then entered a longer period of baseline emissions that remained higher than emissions from soil held in the dark. Baseline emissions from soil samples showed significant variability; however, a relationship with depth is evident in the data (Fig. 7). Neither first- nor second-order kinetic models showed a consistent fit to soil

samples thicker than 4 mm. Thus, the data may suggest a multicomponent model at work in soils whereby one component of the emissions spectrum is limited to the surface of the soil matrix and a second component is driven by a subsurface phenomenon. Both components are driven by exposure to light.

This study was conducted on dry soil, so one limitation of the work is that it does not consider the role that water has in redistributing Hg through the soil system. In addition, speciation of Hg in soil was not considered in this study and could have contributed to the differences in behavior of the soil emission profile compared with sand samples. The analysis and data presented here reflect controlled laboratory conditions and do not take into account other naturally occurring geophysical processes. Given these limitations, these results may suggest that natural processes such as erosion can have a significant effect on soil Hg emissions because they determine when and what layers of soil are exposed to light. This work contributes to our understanding of the kinetics of the processes influencing soil Hg emissions, and we hope that the phenomena observed here can contribute to models aimed at understanding the role of light in the reduction of Hg in soil.

Acknowledgments

Funding for this work was provided by PRISM, a program to support undergraduate research at John Jay College that is funded by the Collegiate Science and Technology Entry Program of the New York State Education Department and the Title V Institutional Development Program of the U.S. Department of Education. Additional funding was provided by a Collaborative Research Incentive Grant from the City University of New York.

References

Almeida, M.D., L.D. Lacerda, W.R. Bastos, and J.C. Herrmann. 2005. Mercury loss from soils following conversion from forest to pasture in Rondônia, Western Amazon, Brazil. Environ. Pollut. 137:179–186.

Bonzongo, J., and A.K. Donkor. 2003. Increasing UV-B radiation at the earth's surface and potential effects on aqueous mercury cycling and toxicity. Chemosphere 52:1263–1273.

Carpi, A., and S.E. Lindberg. 1997. Sunlight-mediated emission of elemental mercury from soil amended with municipal sewage sludge. Environ. Sci. Technol. 31:2085–2091.

Ciavatta, L., and M. Grimaldi. 1968. The hydrolysis of mercury (II) chloride, HgCl2. J. Inorg. Nucl. Chem. 30:563–581.

Divis, P., M. Leermakers, H. Docekalova, and Y. Gao. 2005. Mercury depth profiles in marine sediments measured by the diffusive gradients in thin films technique with two different specific resins. Anal. Bioanal. Chem. 382:1715–1719.

Dreher, G.B., and L.R. Follmer. 2004. Mercury content of Illinois soils. Water Air Soil Pollut. 156:299–325.

Feng, X., G. Li, and G. Qiu. 2006. A preliminary study on mercury contamination to the environment from artisanal zinc smelting using indigenous methods in Hezhang County, Guizhou, China: Part 2. Mercury contaminations to soil and crop. Sci. Total Environ. 368:47–55.

Fitzgerald, W.F., D.R. Engstrom, R. Mason, and E.A. Nater. 1998. The case for atmospheric mercury contamination in remote areas. Environ. Sci. Technol. 32:1–7.

Gomoiu, M.T. 1967. Some quantitative data on light penetration in sediments. Helgol. Mar. Res. 15:120–127.

Gustin, M.S., H. Biester, and C.S. Kim. 2002. Investigation of the light-enhanced emission of mercury from naturally enriched substrates. Atmos. Environ. 36:3241–3254.

Hintelmann, H., R. Harris, A. Heyes, J.P. Hurley, C.A. Kelly, D.P. Krabbenhoft, S. Lindberg, J.W. Rudd, K.J. Scott, V.L. St. Louis. 2002. Reactivity and mobility of new and old mercury deposition in a boreal forest ecosystem during the first year of the METAALICUS study. Environ. Sci. Technol. 36:5034–5040.

Lindberg, S.E., and T.P. Meyers. 2001. Development of an automated micrometerological method for measuring the emission of mercury vapor from wetland vegetation. Wetlands Ecol. Manage. 9:333–347.

Lindberg, S.E., and J. Price. 1999. Measurements of the airborne emission of mercury from municipal landfill operations: A short term study in Florida. J. Air Waste Manage. Assoc. 49:174–185.

Mauclair, C., J. Layshock, and A. Carpi. 2008. Quantifying the effect of humic matter on the emission of mercury from artificial soil surfaces. Appl. Geochem. 23:594–601.

Moore, C., and A. Carpi. 2005. Mechanisms of the emission of mercury from soil: Role of UV radiation. J. Geophys. Res. 110:D24302, doi:10.1029/2004JD005567.

Schlüter, K. 2000. Review: Evaporation of mercury from soils. An integration and synthesis of current knowledge. Environ. Geol. 39:249–271.

Schlüter, K., H.M. Seip and J. Alstad. 1995. Mercury translocation in and evaporation from soil II: Evaporation of mercury from podzolized soil profiles treated with $HgCl_2$ and CH_3CHCl. J. Soil Contam. 4:269–298.

Schuster, E. 1991. The behavior of mercury in the soil with special emphasis on complexation and adsorption processes: A review of the literature. Water Air Soil Pollut. 56:667–680.

Siegel, S.M., and B.Z. Siegel. 1988. Temperature determinants of plant-soil-air mercury relationships. Water Air Soil Pollut. 40:443–448.

Song, X., and B. Van Heyst. 2005. Volatilization of mercury from soils in response to simulated precipitation. Atmos. Environ. 39:7494–7505.

USDA. 2010. Custom soil resource report for State of Connecticut. Web soil survey for Fairfield County. Available at http://websoilsurvey.nrcs.usda.gov/app/WebSoilSurvey.aspx (verified 14 Jan. 2011).

Wang, D., X. Shi, and S. Wei. 2003. Accumulation and transformation of atmospheric mercury in soil. Sci. Total Environ. 304:209–214.

Wood, J.M. 1974. Biological cycles for toxic elements in the environment. Science 183:1049–1052.

Xin, M., M. Gustin, and D. Johnson. 2007. Laboratory investigation of the potential for re-emission of atmospherically derived Hg from soils. Environ. Sci. Technol. 41:4946–4951.

Zhang, H., S.E. Lindberg, F.J. Marsik, and G.J. Keeler. 2001. Mercury air/surface exhange kinetics of background soils of the Tahquamenon river watershed in the Michigan upper peninsula. Water Air Soil Pollut. 126:151–169.